

The Potential Use of Zeolite, Montmorillonite, and Biochar for the Removal of Radium-226 from Aqueous Solutions and Contaminated Groundwater

Authors:

Fahad I. Almasoud, Abdullah S. Al-Farraj, Mohammad I. Al-Wabel, Adel R.A. Usman, Yousef J. Alanazi, Zaid Q. Ababneh

Date Submitted: 2021-06-21

Keywords: kinetics, adsorption isotherms, groundwater remediation, removal efficiency, 226Ra, zeolite

Abstract:

The present work investigated the potential of using zeolite (clinoptilolite), montmorillonite (Swy2), and Conocarpus biochar as adsorbents to remove 226Ra from aqueous solution. The effect of the initial 226Ra concentrations on sorbents' equilibrium activity concentrations and sorbents' radium removal efficiency were investigated. The results showed that zeolite has a higher removal efficiency for 226Ra in comparison with the efficiencies of montmorillonite and biochar. In addition to the linear isotherm model, the Freundlich model, followed by Temkin's model, provided a better description of the adsorption process than the Langmuir model. Kinetic studies indicated that a pseudo-second-order kinetic model could be the best fit for the adsorption of 226Ra onto the three investigated sorbents, which suggests that the mechanism of adsorption of 226Ra by sorbents was chemisorption. The intraparticle diffusion model indicated that adsorption of 226Ra onto the sorbents involves a multistep process: (i) boundary layer diffusion and (ii) intraparticle diffusion. Moreover, the remediation of groundwater samples polluted with 226Ra was assessed using the investigated sorbents; the results showed that zeolite also has the highest removal efficiency among other sorbents. Thus, the low cost, availability, and the high adsorption efficiency of zeolite can be a promising sorbent on 226Ra removal from aqueous solutions and groundwater remediation.

Record Type: Published Article

Submitted To: LAPSE (Living Archive for Process Systems Engineering)

Citation (overall record, always the latest version):

LAPSE:2021.0539

Citation (this specific file, latest version):

LAPSE:2021.0539-1

Citation (this specific file, this version):





LAPSE:2021.0539-1v1

DOI of Published Version: <https://doi.org/10.3390/pr8121537>

License: Creative Commons Attribution 4.0 International (CC BY 4.0)

Article

The Potential Use of Zeolite, Montmorillonite, and Biochar for the Removal of Radium-226 from Aqueous Solutions and Contaminated Groundwater

Fahad I. Almasoud ^{1,2,*}, Abdullah S. Al-Farraj ², Mohammad I. Al-Wabel ²,
Adel R.A. Usman ^{2,3,*}, Yousef J. Alanazi ⁴ and Zaid Q. Ababneh ^{5,6}

¹ Nuclear Science Research Institute (NSRI), King Abdulaziz City for Science and Technology (KACST), P.O. Box 6086, Riyadh 11442, Saudi Arabia

² Department of Soil Sciences, College of Food and Agricultural Sciences, King Saud University, P.O. Box 2460, Riyadh 11451, Saudi Arabia; sfarraj@ksu.edu.sa (A.S.A.-F.); malwabel@ksu.edu.sa (M.I.A.-W.)

³ Department of Soils and Water, Faculty of Agriculture, Assiut University, Assiut 71526, Egypt

⁴ Nuclear and Radiological Regulatory Commission (NRRRC), Riyadh 12244, Saudi Arabia; yalanazi@nrrc.gov.sa

⁵ Physics Department., Faculty of Science, Yarmouk University, Irbid 211-63, Jordan; zababneh@yu.edu.jo

⁶ College of Applied Medical Sciences, King Saud bin Abdulaziz University for Health Sciences, P.O. Box 6664, Al-Ahsa 31982, Saudi Arabia

* Correspondence: fmasaud@kacst.edu.sa or fmasaud@gmail.com (F.I.A.); adosman@ksu.edu.sa (A.R.A.U.); Tel.: +966-114-813-629 (F.I.A.); +966-114699784 (A.R.A.U.); Fax: +966-114-814-750 (F.I.A.); +966-114678440 (A.R.A.U.)

Received: 30 October 2020; Accepted: 22 November 2020; Published: 25 November 2020



Abstract: The present work investigated the potential of using zeolite (clinoptilolite), montmorillonite (Swy2), and *Conocarpus* biochar as adsorbents to remove ²²⁶Ra from aqueous solution. The effect of the initial ²²⁶Ra concentrations on sorbents' equilibrium activity concentrations and sorbents' radium removal efficiency were investigated. The results showed that zeolite has a higher removal efficiency for ²²⁶Ra in comparison with the efficiencies of montmorillonite and biochar. In addition to the linear isotherm model, the Freundlich model, followed by Temkin's model, provided a better description of the adsorption process than the Langmuir model. Kinetic studies indicated that a pseudo-second-order kinetic model could be the best fit for the adsorption of ²²⁶Ra onto the three investigated sorbents, which suggests that the mechanism of adsorption of ²²⁶Ra by sorbents was chemisorption. The intraparticle diffusion model indicated that adsorption of ²²⁶Ra onto the sorbents involves a multistep process: (i) boundary layer diffusion and (ii) intraparticle diffusion. Moreover, the remediation of groundwater samples polluted with ²²⁶Ra was assessed using the investigated sorbents; the results showed that zeolite also has the highest removal efficiency among other sorbents. Thus, the low cost, availability, and the high adsorption efficiency of zeolite can be a promising sorbent on ²²⁶Ra removal from aqueous solutions and groundwater remediation.

Keywords: zeolite; ²²⁶Ra; removal efficiency; groundwater remediation; adsorption isotherms; kinetics

1. Introduction

In a broad sense, water resources have been subject to pollution from the increases in concentrations of both heavy metals and natural radionuclides. Radium is considered one of the most naturally occurring radionuclides that exist in appreciable amounts in water and groundwater in particular. The amount of ²²⁶Ra in groundwater depends on the type of bedrock structure and its interaction with

the groundwater and the prolonged contact between these rocks and groundwater. Thus, water hosted within igneous rocks has a higher radium concentration than those hosted within sedimentary rocks [1,2]. Human activities can also result in the elevation of radium in the environment, which ultimately reaches surface water and groundwater. Such activities include the production of the oil and gas industry [3,4], uranium mining [5], and phosphate fertilizers [6].

The presence of radium at a higher level in the water and its associated health impact on humans has received considerable attention from researchers in the last few decades. The importance of radium comes from the fact that it is one of the most natural radiotoxic radionuclides that emit alpha particles with relatively high linear energy transfer; thus, ingestion of drinking water that contains a high level of radium increases genetic damage, which may lead to cancer, particularly bone cancer, in humans [7,8]. Therefore, several national and international authorities set limits of radionuclides in drinking water. For example, the Environmental Protection Agency (EPA) regulates the combined radium ($^{228}\text{Ra} + ^{226}\text{Ra}$) in drinking water so that it is less than 0.185 Bq/L (5 pCi/L) [9].

Several studies have been conducted worldwide, including in Saudi Arabia, to investigate the naturally occurring radioactive materials (NORMs) in groundwater [10–16]. To a large extent, most of these studies showed that groundwater contains a significant level of natural radionuclides, especially radium. In Saudi Arabia, in addition to desalination water, groundwater is considered one of the primary sources of drinking water. It contributes almost 40% of the drinking water in the country [17]. Thus, the elevated level of natural radionuclides in drinking water can be considered as the primary source of contamination. Moreover, Saudi Arabia is characterized by a semiarid to an arid climate, which results in water scarcity. Therefore, the agricultural crops of the farms are mainly irrigated from groundwater, which contains an appreciable number of NORMs. Consequently, this will increase the accumulation of NORM in the soil, which ultimately reaches the human body via soil to plant transfer [18]. Thus, it has become important to carry out radionuclide remediation for the contaminated soil by applying a fixation process for these radionuclides in the soil by using clay minerals.

Hence, water pollution due to radionuclides is a global issue. Therefore, several methods have been employed for removing radionuclides from water, including radium. Such methods include chemical precipitation, reverse osmosis, ion exchange, and lime softening. In these methods, the radium removal efficiency from water can reach up to 95% [19].

In recent years, other attractive methods have been used to remove radionuclides from aqueous solutions based on adsorption of the radionuclides from water by applying different natural adsorbents, such as clays, bentonite, and zeolites [20–23]. The low cost of these natural adsorbents, their availability, high removal efficiency, which could reach almost 100%, and high sorption properties make them attractive to use in water purification from radioactive and other heavy elements.

Among the natural materials, zeolite has been widely used as a natural sorbent to absorb radionuclides and heavy elements from aqueous solutions, mine water, and soil [20,22,24–26]. This is due to the unique porous structure of zeolites, which are classified as aluminosilicate minerals with high ion exchange and sorption properties.

Most radioactivity studies in Kingdom of Saudi Arabia (KSA) showed a high concentration of ^{226}Ra in groundwater, and the crops irrigated from this groundwater. Thus, it is imperative to carry out radionuclide remediation for both contaminated soil and water. Therefore, several available natural materials such as zeolite, montmorillonite, and biochar have been proposed for this issue.

This study aimed to investigate the potential use of zeolite, montmorillonite, and biochar to remove ^{226}Ra from aqueous solutions and groundwater in terms of adsorption isotherms kinetics. In addition, ^{226}Ra adsorption by sandy soil amended with zeolite was investigated.

2. Materials and Methods

2.1. Sample Preparation

In this work, the natural zeolite used was clinoptilolite (Morgan Co., Morgan, Mountain Green, UT, USA). The montmorillonite (SWy2) was purchased from the Clay Mineral Society (West Lafayette, IN, USA), while the biochar was produced after pyrolyzing the chopped *Conocarpus* wood wastes at 400 °C using a closed system, which is made of stainless steel (height of 22 cm and diameter of 7 cm), for 4 h. The results showed that the *Conocarpus* biochar has an alkaline pH of 9.67. The detailed characteristics of the produced biochar were presented by Al-Wabel and Al-Omran [27]. The surface area and pore size characteristics of each investigated adsorbent were determined by surface area and a pore size analyzer (NOVA touch LX4, Quantachrome Instruments, Graz, Austria). The surface area, pore volume, and pore radius of each adsorbent are listed in Table 1.

Table 1. The values of surface area, pore volume, and pore radius for each investigated adsorbent.

Sorbent	BET Surface Area (m ² g ⁻¹)	Pore Radius (nm)	Total Pore Volume (cc g ⁻¹)
Zeolite	44.3868	1.460	0.066
montmorillonite	38.1534	1.330	0.045
Biochar	54.3115	1.510	0.059

BET: Brunauer–Emmett–Teller.

A bottle of one liter of distilled water was spiked with a high-purity ²²⁶Ra standard from the National Institute for Standard Technology (NIST), USA, with the known activity concentration to get four standards with activity concentrations of 1, 3, 5, and 7 Bq L⁻¹.

All the standard sources were homogenized. A total of 25 mL of the standard source was taken, with a mass of 0.5 g, from all sorbent materials used for the removal of ²²⁶Ra from the aqueous solutions and were then shaken for 24 h. Subsequently, the solutions were filtered by Whatman 45 mm.

2.2. Samples Measurement

An 8 mL of the filtered solution was transferred in a high-density polyethylene vial (size 20 mL) with a Teflon cap to prevent radon from escaping. Each of the standard solutions were then added with 12 mL of a high-efficiency mineral oil scintillator cocktail (PerkinElmer, Boston, MA, USA). Afterward, all samples were stored in a refrigerator for at least 30 days to establish a secular equilibrium between ²²²Rn and ²²⁶Ra and their respective decay products before the measurement of the radioactivity using a Liquid Scintillation Counter, Quantulus 1220 Ultra-low-level background (LSC) (PerkinElmer, Turku, Finland).

The LSC equipped with a pulse-shaped analyzer that has the proper setting of the α/β discrimination parameter. The stability study of the detector was carried out by using two standards sources, supplied by PerkinElmer (Turku, Finland) covering high energy beta ¹⁴C and low energy beta ³H. The calibration was conducted with an in-house mixed standard source containing pure alpha (²⁴¹Am) and pure beta ⁹⁰Sr emitters, which were obtained from the National Institute for Standard Technology (NIST), USA. The window setting in the LSC of ²²⁶Ra was conducted by a standard source of ²²⁶Ra obtained from the NIST. The lower limit detection (LLD) was calculated by Curie equation, and the activity concentration was found to be 0.07, 0.32, and 0.08 Bq L⁻¹ for alpha, beta, and ²²⁶Ra, respectively. The LLD was achieved under the following conditions: 8 mL sample size, 500 min of counting time, and efficiency of 99% [16,28–32].

2.3. Adsorption Isotherm Analysis

The ²²⁶Ra equilibrium adsorption was described by using the isotherm models of linear form and the nonlinear form of Langmuir, Freundlich, and Temkin. The equations of isotherms are shown below.

The linear isotherm equation is given below

$$q_e = k_d C_e \quad (1)$$

where the q_e is the quantity of ^{226}Ra adsorbed on different adsorbent at equilibrium (Bq g^{-1}), C_e is the ^{226}Ra concentration at equilibrium in solution phase (Bq L^{-1}), and k_d is the linear adsorption constant.

The Langmuir isotherm equation in its linear form is given below

$$\frac{C_e}{q_e} = \frac{1}{k_l q_m} + \frac{C_e}{q_m} \quad (2)$$

where q_m is the maximum quantity of ^{226}Ra adsorbed on different adsorbent at saturation (Bq g^{-1}), and k_l (L Bq^{-1}) is the Langmuir constant, which is related to enthalpy.

The linear Freundlich isotherm equation is as follows:

$$\log q_e = \log k_f + \left(\frac{1}{n}\right) \log C_e \quad (3)$$

where k_f is the Freundlich constant, which represents the adsorption capacity, and $1/n$ is the adsorption intensity related to surface heterogeneity of the adsorbent.

The linear form of Temkin isotherm is expressed as follows:

$$q_e = B_T \ln(A_T) + B_T \ln(C_e) \quad (4)$$

$$B_T = \frac{RT}{b_T}$$

where (A_T) is Temkin isotherm equilibrium binding constant (L g^{-1}); B_T is constant related to the heat of sorption (J/mol); b_T is Temkin isotherm constant; R is the universal gas constant, and T is the temperature at 298 K.

To evaluate the goodness of fit for the applied isotherm models, the sum of the squares of the errors (SSE), residual root mean square error (RSME), and Chi-square (χ^2) test were computed as follows:

$$\text{SSE} = \sum_{i=1}^n (q_e - q_{e,m})^2 \quad (5)$$

$$\text{RSME} = \sqrt{\sum_{i=1}^n (q_e - q_{e,m})^2} \quad (6)$$

$$\chi^2 = \sum \frac{(q_e - q_{e,m})^2}{q_{e,m}} \quad (7)$$

where $q_{e,m}$ is the equilibrium capacity obtained by calculating from the model (mg g^{-1}), and q_e is experimental data of the equilibrium capacity (mg g^{-1}).

2.4. Adsorption Kinetic Analysis

In order to investigate the mechanisms of adsorption of ^{226}Ra onto the investigated sorbents, several kinetics models were used, including first-order, second-order, pseudo-second-order, Elovich, power function, and intraparticle diffusion kinetic models.

First-order equation:

$$\ln q_t = \ln q_e - k_1 t \quad (8)$$

Second-order equation:

$$\frac{1}{q_t} = \frac{1}{q_e} + K_2 t \quad (9)$$

Pseudo-second-order equation:

$$\frac{1}{q_t} = \frac{1}{k_2 t q_e^2} + \frac{1}{q_e} \quad (10)$$

Power function equation:

$$\ln q_t = \ln b + k_f (\ln t) \quad (11)$$

Elovich equation:

$$q_t = \frac{\ln(\alpha\beta)}{\beta} + \frac{\ln(t)}{\beta} \quad (12)$$

Intraparticle diffusion equation:

$$q_t = a + k_{id}t^{0.5} \quad (13)$$

where q_t and q_e are the amount of ^{226}Ra adsorbed by different sorbent (Bq g^{-1}) at any time t (min), and at equilibrium, respectively. k_1 is the adsorption rate constant in the first-order model; K_2 is the adsorption rate constant in the second-order model ($\text{g Bq}^{-1} \text{min}^{-1}$); k_2 is the rate constant of pseudo-second-order absorption ($\text{g Bq}^{-1} \text{min}^{-1}$); k_f is the rate constant of power function adsorption ($\text{Bq g}^{-1} \text{min}^{-1}$); α is the initial adsorption rate ($\text{Bq g}^{-1} \text{min}^{-1}$); β is Elovich constant (g Bq^{-1}); a and b are constants; k_{id} is the intraparticle diffusion rate constant ($\text{Bq g}^{-1} \text{min}^{-0.5}$).

3. Results and Discussion

3.1. Adsorption Isotherms of ^{226}Ra onto Sorbents

Studies on the adsorption isotherm of ^{226}Ra on the investigated adsorbents were carried out at an initial pH value of 5, sorbent dose 20 g L^{-1} , and for initial concentration of ^{226}Ra (1,3,5,7) Bq L^{-1} . The ^{226}Ra equilibrium adsorption isotherms were shown in Figure 1. The results show that adsorption of ^{226}Ra by zeolite, montmorillonite, and biochar tended to increase by increasing the initially added activity concentrations of ^{226}Ra . It was observed that the adsorption of ^{226}Ra onto zeolite shows a different behavior than its adsorption onto montmorillonite and biochar. In general, adsorption of ^{226}Ra to zeolite was characterized by the Giles adsorption isotherm classification H-type, indicating high affinity overall added initial concentrations. Meanwhile, adsorption of ^{226}Ra to montmorillonite and biochar was characterized by the Giles adsorption isotherm classification C-type, indicating constant partition. The isotherm shapes indicate that the zeolite has a higher potential for ^{226}Ra adsorption in comparison with those of montmorillonite and biochar [33]. It has been previously reported that natural zeolite with a porous structure and molecular sieves is a promising tool to remediate radium isotopes from waste mine water [20].

The experimental equilibrium data obtained were analyzed using regression models of isotherms Linear, Langmuir, Freundlich, and Temkin, and their various parameters are shown in Table 2. Linear regression analysis for the Langmuir and Freundlich isotherms is commonly used for the best isotherm fitting. In the current study, among all models, Langmuir's model did not describe the adsorption of ^{226}Ra on three sorbents with a lower r^2 and higher values of SSE or RSME or X^2 compared to other three applied models (Linear, Freundlich, and Temkin). However, Linear's model well explains the adsorption of ^{226}Ra on three sorbents with a higher r^2 of 0.9875, 0.9998, and 0.9898, respectively, for zeolite, montmorillonite, and biochar. The zeolite showed a much higher Linear distribution coefficient (k_d) value (4.44) for ^{226}Ra adsorption than the other two sorbents (0.086 for montmorillonite; 0.022 for biochar). Additionally, Freundlich's model showed a good explanation for the adsorption of ^{226}Ra on three sorbents with r^2 of 0.9289, 0.9998, and 0.9955, respectively, for zeolite, montmorillonite, and biochar. The explained data by Freundlich's model suggest that the adsorption was not uniform site rather than multilayer adsorption, and it was rather heterogeneous than homogeneous. Overall, the Freundlich coefficient values ($1/n$) were below 1 for montmorillonite and biochar (but not for zeolite), indicating favorable adsorption of ^{226}Ra to the sorbents, especially for montmorillonite and biochar. In addition, the zeolite showed a much higher k_f value for ^{226}Ra adsorption than others. Temkin models

with r^2 of 0.9130–0.9970 can also describe the adsorption of ^{226}Ra onto the investigated sorbents. The fit of ^{226}Ra adsorption onto the sorbents to Temkin models suggests a chemical adsorption mechanism with physical forces. Among three sorbents, zeolite showed much higher Temkin equilibrium binding (A_T) and adsorption constants (b_T) as well as a constant relative to the heat adsorption (B_T).

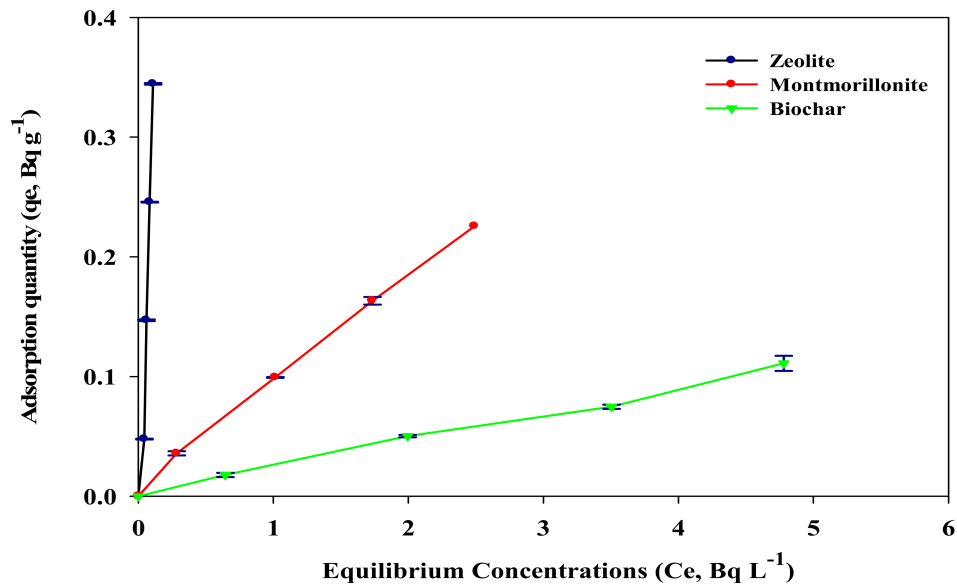


Figure 1. The ^{226}Ra equilibrium adsorption isotherms for the investigated sorbents (at pH = 5, sorbent dose 20 g L^{-1} , and initial concentration of ^{226}Ra (1,3,5,7) Bq L^{-1}).

Table 2. The Linear, Langmuir, Freundlich, and Temkin isotherm parameters for ^{226}Ra adsorption.

Model	Parameters	Sorbents		
		Zeolite	Montmorillonite	Biochar
Linear	r^2	0.9875	0.9998	0.9898
	k_d	4.44	0.086	0.022
	χ^2	0.00722	3.39×10^{-5}	0.00070
	SSE	0.00061	4.79×10^{-6}	4.75×10^{-5}
	RSME	0.025	0.002	0.0069
Langmuir	r^2	0.6118	0.8155	0.6371
	q_m	-0.124	0.765	0.498
	k_l	7.27	0.16	0.056
	χ^2	0.0962	0.0011	0.00096
	SSE	0.0278	0.0001	8.33×10^{-5}
Freundlich	r^2	0.9289	0.9988	0.9955
	k_f	43.33	0.102	0.0263
	$1/n$	2.13	0.848	0.892
	χ^2	0.0216	0.00026	0.0007
	SSE	0.0046	3.74×10^{-5}	5.9×10^{-5}
Temkin	r^2	0.9970	0.9195	0.9130
	A_T	25.78	4.61	2.05
	B_T	0.3255	0.0826	0.0427
	χ^2	0.00063	0.0158	0.0067
	SSE	0.0001	0.0016	0.0004
	RSME	0.0120	0.0402	0.0201

The removal efficiency of sorbents for ^{226}Ra in relation to the initial added concentrations is shown in Table 3. The percentage removal of ^{226}Ra was affected by sorbent type and initial activity. The highest removal efficiency values were pronounced for ^{226}Ra adsorption onto zeolite. The percentage removal of ^{226}Ra onto zeolite increased as the initial ^{226}Ra activity concentration was increased, but the percentage removal of ^{226}Ra onto montmorillonite and biochar tended to decrease with increasing initial activity concentration. A similar finding of high removal efficiency for ^{226}Ra in aqueous media (98.73%) was reported by Erenturk and Kaygun [23] when using adsorbent the zeolite clinoptilolite modified by polyacrylonitrile. It has been reported previously that partition coefficient (PC) can be applied for determining the performance of different sorbents, mainly to minimize the bias of the adsorption capacity concepts [34]. Therefore, to compare the performance of the synthesized sorbents, the PCs were calculated. Table 3 shows the partition coefficient PC values in relation with the initial added activity concentration of ^{226}Ra . The highest PC values were pronounced for ^{226}Ra adsorption onto zeolite (PC of 1061–3132 L kg⁻¹), indicating a high reduction in ^{226}Ra activity by the solid phase of zeolite. Overall, the lowest PC values were more pronounced for the biochar (PC = 21.3–27.5 L kg⁻¹) and followed by montmorillonite (PC = 90.6–125 L kg⁻¹). It was observed that PC values for adsorption of ^{226}Ra onto zeolite tended to increase with the increasing initial activity concentration. The higher PC values that were observed for higher initial activity concentrations are mainly explained by the available sites of high selectivity and strong bonding energies for zeolite. However, the lower PC values with decreasing initial activity concentrations indicate that energetically less favourable sites with decreasing activity of ^{226}Ra .

Table 3. Sorbent effects on equilibrium activity concentrations, removal efficiency and partition coefficient of ^{226}Ra in aqueous solutions.

Sorbent Type	Initial Concentrations, (Bq L ⁻¹)	Equilibrium Activity Concentrations, (Bq L ⁻¹)	Removal Efficiency (%)	Partition Coefficient (PC, L kg ⁻¹)
Zeolite	1	0.045	95.50	1061
	3	0.060	98.00	2450
	5	0.085	98.30	2891
	7	0.110	98.43	3132
Montmorillonite	1	0.285	71.50	125.0
	3	1.015	66.17	97.80
	5	1.735	65.30	94.10
	7	2.490	64.43	90.60
Biochar	1	0.65	35.50	27.50
	3	2.00	33.50	25.20
	5	3.51	29.90	21.30
	7	4.78	31.71	23.20

Though previous studies demonstrated that biochar has the potential to remove heavy metals from aqueous solutions [35,36], the obtained results from the current study indicate that biochar has less ability to remove radioactive ^{226}Ra .

3.2. Adsorption Kinetics of ^{226}Ra onto Sorbents

In the current study, adsorption kinetics of ^{226}Ra onto zeolite, montmorillonite, and biochar were investigated by using the model of the first-order, second-order, pseudo-second-order, Elovich, power function, and intraparticle diffusion kinetic models. Kinetics of ^{226}Ra removal onto each sorbent were investigated for time interval range from 60 to 1440 min using a Mechanical shaker at 150 rounds per minute (rpm), initial activity concentration 5 Bq L⁻¹, sorbent dose 20 g L⁻¹ at an initial pH value of 5. The results are shown in Figure 2. Additionally, the determined parameters of the best one models studied (pseudo-second-order) for ^{226}Ra are presented in Table 4. ^{226}Ra adsorption by zeolite was faster than montmorillonite and followed by biochar in the kinetic adsorption experiment. For example, in the first 60 min, most adsorbed quantity (98.3% uptake) was observed, and then, the adsorbed quantity showed a little increase (99.0–99.8% uptake) with increasing equilibrium kinetic time of 120–1140 min. However, for montmorillonite, in 60, 120, and 240 min, respectively,

the adsorbed quantity amounted to 65.3, 75.6, and 83.4% uptake), and then, the adsorbed quantity showed an increase of 90.2–94.80% uptake with increasing equilibrium kinetic time of 480–1140 min. Among all sorbents, biochar showed the slower ^{226}Ra adsorption, which accounted for 29.9 (at 60 min), 48.0 (at 120 min), 66.7 (at 240 min), 75.8 (at 480 min), 83.8 (at 960 min), 86.2% uptake (1440 min). Among all applied adsorption kinetic models, the pseudo-second-order kinetic's model well explains the adsorption data of ^{226}Ra . It was found that the pseudo-second-order kinetic model provided higher correlation coefficients with experimental results (r^2 of 1.000 for zeolite, 0.9999 for montmorillonite, and 0.9996 for biochar; Table 4), speculating chemisorption of the ^{226}Ra onto the sorbents. The q_e values of ^{226}Ra derived from pseudo-second-order kinetic were 0.250, 0.242 and 0.233 Bq g^{-1} for zeolite, montmorillonite, and biochar, respectively. Meanwhile, the k_2 values of the pseudo-second-order kinetic amounted to 3.665, 0.121, and 0.039 for zeolite, montmorillonite, and biochar, respectively. Among all sorbents, the highest q_e and k_2 values were pronounced for zeolite. The value of q_e obtained from the pseudo-second-order kinetic model for zeolite is identical to that of the experimental value. As indicated by Houhoune Khemaissia [37], the pseudo-second-order model has successfully described radioactive metals onto sorbents. Our findings generally suggest that the rate-controlling mechanism might be chemisorption, indicating the sharing or exchange of electrons between ^{226}Ra and zeolite.

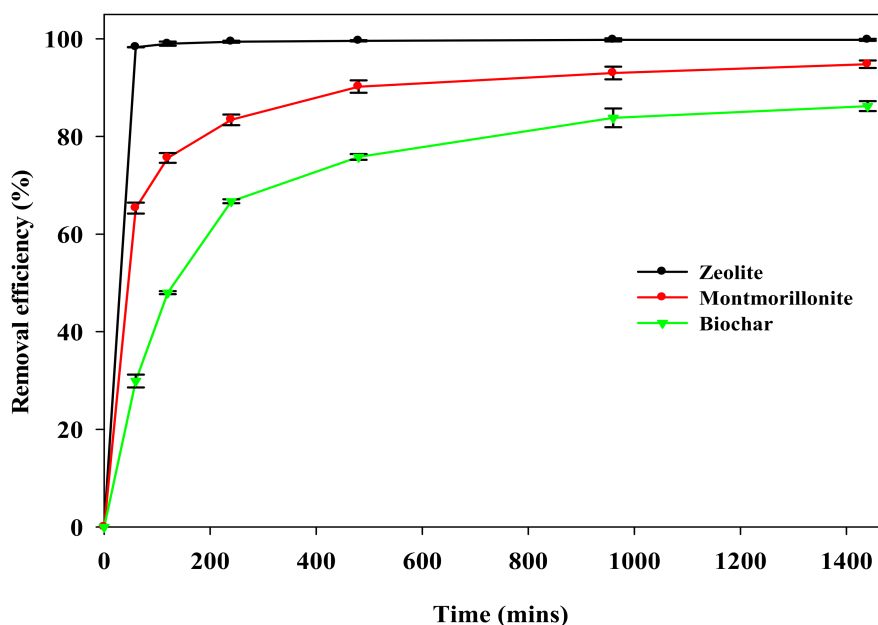


Figure 2. Kinetics of ^{226}Ra removal onto three investigated sorbents (at initial activity concentration 5 Bq L^{-1} , sorbent dose 20 g L^{-1} , and $\text{pH} = 5$).

However, the pseudo-second-order kinetics might provide many sorption steps, including external film diffusion, sorption, and internal particle diffusion. In addition, this model cannot explain the specific sorption mechanism. Therefore, the intraparticle diffusion kinetic model was applied to the data of this study. Several studies showed that the intraparticle diffusion plot might represent multilinearity, indicating that two or more steps could occur. The results showed that the data points mostly have two straight lines, and the plots did not pass through the origin (Figure 3). Table 4 shows that the k_{i2} values were smaller than the k_{i1} values, suggesting that the intraparticle diffusion was predicted to be the rate-limiting step for the ^{226}Ra adsorption onto the three investigated sorbents. In this study, the deflection of the straight lines from the origin indicated that the intraparticle diffusion is not only the rate-limiting step in the process of ^{226}Ra onto the investigated sorbents, and other kinetic models, such as surface adsorption, may control the rate of adsorption. Generally, the kinetic data indicated that the mechanism of ^{226}Ra adsorption by zeolite, montmorillonite, or biochar is complex and can probably occur through a combination process including external mass transfer, intraparticle

diffusion through the macropores and micropores as well as sorption processes. It should also be noted that the kinetic process fitted by the pseudo-second-order model suggests chemisorption. In the case of the rate-limited chemisorption, the inner-sphere complexation involved the radioactive metal ions' sorption.

Table 4. Kinetic parameters for ^{226}Ra adsorption models.

Model	Parameters	Sorbents		
		Zeolite	Montmorillonite	Biochar
Pseudo-second-order	H	0.228	0.007	0.002
	k_2	3.665	0.121	0.039
	q_e	0.250	0.242	0.233
	r^2	1.000	0.9999	0.9996
Initial first linear portion (Intraparticle diffusion)	k_{id1}	0.0003	0.0042	0.0118
	a_1	0.243	0.1337	-0.0137
	r^2	0.9364	0.9407	0.9921
Initial second linear portion (Intraparticle diffusion)	K_{id2}	5.0×10^{-5}	0.0007	0.0016
	a_2	0.248	0.2099	0.1549
	r^2	0.8940	0.9976	0.9500

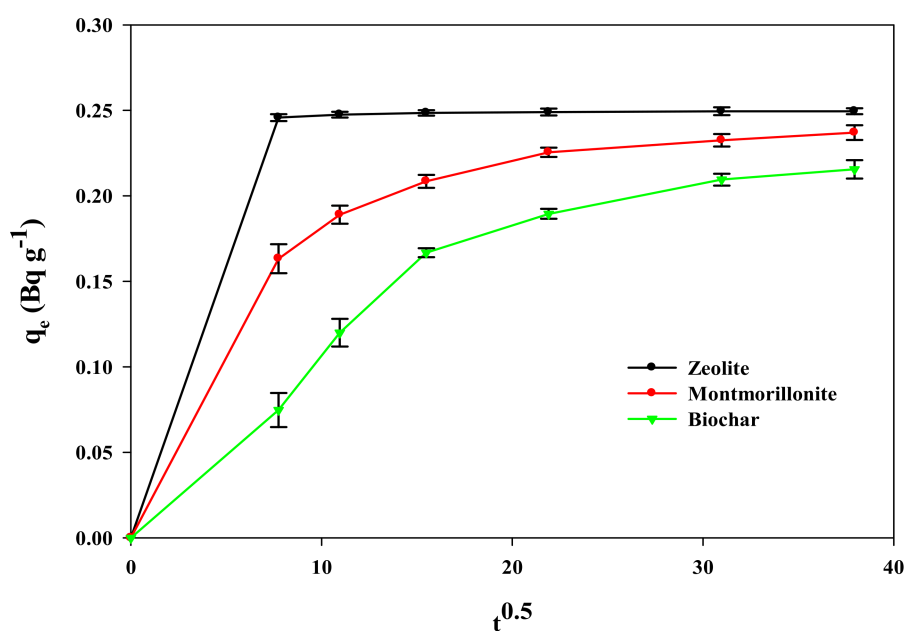


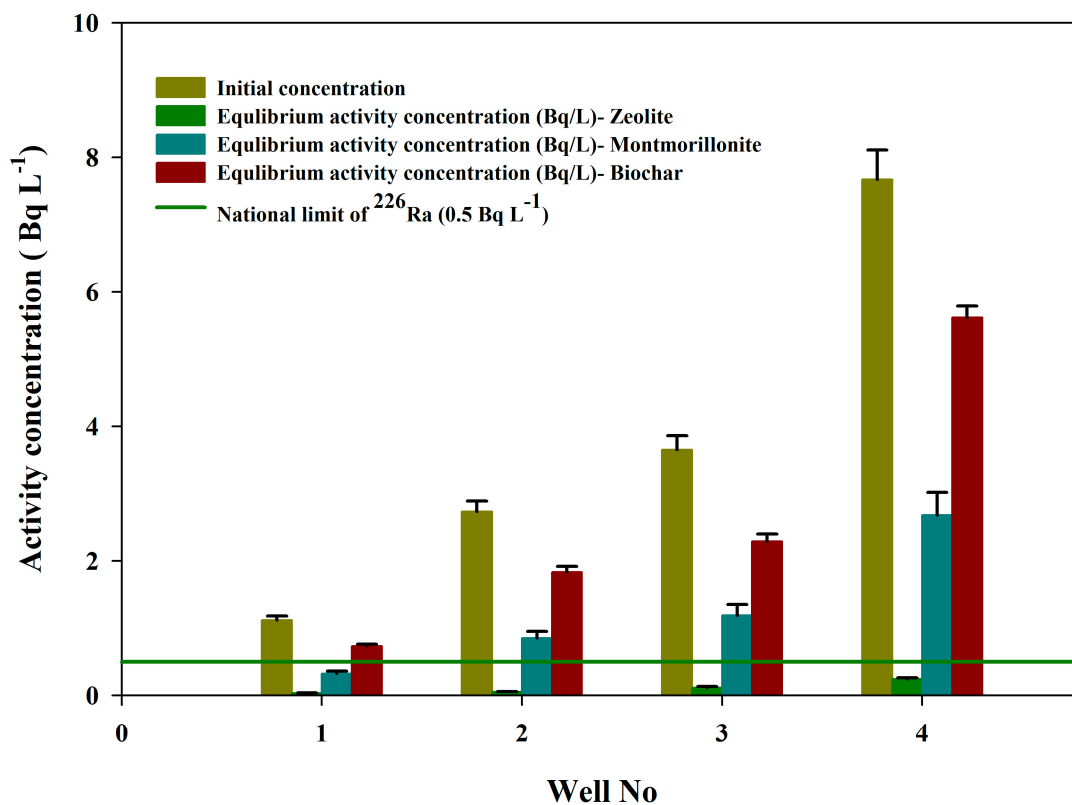
Figure 3. The ^{226}Ra adsorption onto the three investigated sorbents based on the intraparticle diffusion kinetic model.

3.3. The Sorbent Potential for Groundwater Remediation

The activity concentrations of ^{226}Ra in collected groundwater samples ranged from 1.12 to 7.67 Bq L^{-1} (Table 5), which are higher than their corresponding permissible activity concentrations 0.5 Bq L^{-1} in water for drinking purposes [38]. After the treatment of groundwater samples with the investigated sorbents, the activity concentrations of ^{226}Ra in groundwater samples reduced from 1.12–7.68 Bq L^{-1} to 0.04–0.23 Bq L^{-1} for zeolite, to 0.32–2.68 Bq L^{-1} for montmorillonite, and 0.74–5.63 Bq L^{-1} for biochar (Figure 4).

Table 5. Sorbent effects on equilibrium activity concentrations and removal efficiency of contaminated groundwater.

Order of Groundwater Wells	Sorbent Type	Initial Concentrations, (Bq L ⁻¹)	Equilibrium Activity Concentrations, (Bq L ⁻¹) (±1σ)	Removal Efficiency (%) (±1σ)
Well-1	Zeolite	1.12	0.04 ± 0.004	96.30 ± 0.01
	Montmorillonite		0.32 ± 0.03	71.73 ± 2.27
	Biochar		0.74 ± 0.09	34.56 ± 1.94
Well-2	Zeolite	2.76	0.06 ± 0.01	97.71 ± 0.10
	Montmorillonite		0.85 ± 0.04	69.04 ± 0.85
	Biochar		1.84 ± 0.06	33.24 ± 1.18
Well-3	Zeolite	3.65	0.12 ± 0.02	96.81 ± 0.28
	Montmorillonite		1.19 ± 0.08	67.54 ± 1.25
	Biochar		2.29 ± 0.10	37.33 ± 0.87
Well-4	Zeolite	7.68	0.23 ± 0.02	97.07 ± 0.17
	Montmorillonite		2.68 ± 0.07	68.08 ± 0.31
	Biochar		5.63 ± 0.05	26.71 ± 0.26

**Figure 4.** Equilibrium concentrations of ²²⁶Ra in groundwater samples as affected by the three investigated sorbents.

Among all sorbents, zeolite showed the highest removal efficiency, and thus reduced the activity concentrations of ²²⁶Ra in all investigated groundwater samples to less than 0.5 Bq L⁻¹ (permissible concentrations for drinking water) (Figure 4). Previously, it has been reported that natural zeolites have already been identified as a significant tool for environmental remediation [39]. Mostly, it is focused on the ion exchange properties of zeolite. Zeolites with many exchangeable sites and small pores are suitable for processes of sorption [26]. Therefore, it has been reported that zeolites are useful for the removal of radioisotopes from aqueous nuclear wastes [40,41].

3.4. ^{226}Ra Adsorption by Sandy Soil Amended with Zeolite

After mixing zeolite in sandy soil for 21 days, the ^{226}Ra adsorption was carried out with an initial activity concentration of 5.0 Bq L^{-1} . In Figure 5, considering the control of sandy soil (without the addition of zeolite), the removal efficiency of ^{226}Ra accounted for 18%. Meanwhile, after mixing zeolite in sandy soil, the removal efficiency for ^{226}Ra showed significant increases. The results showed that the removal efficiency of ^{226}Ra increased from 18% in control soil to 73, 88, 94, 96, 98% in soil treated with zeolite at an application rate of 1, 5, 10, 15 and 20% (w/w), respectively.

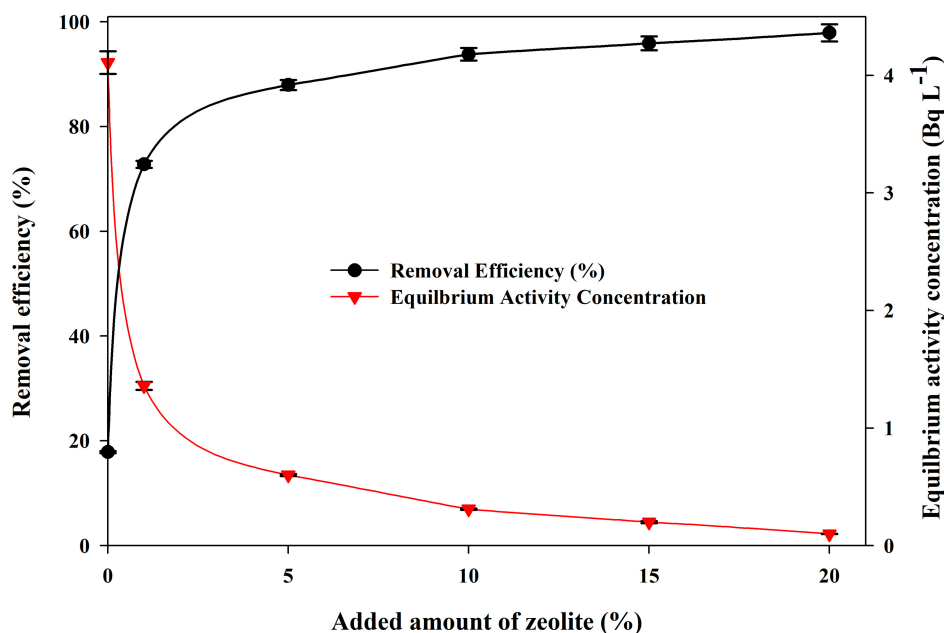


Figure 5. The adsorption efficiency of ^{226}Ra by sandy soil amended with zeolite.

3.5. Mechanism of ^{226}Ra Adsorption onto Natural Zeolite (Clinoptilolite)

The kinetic study showed that the obtained data of ^{226}Ra adsorption onto zeolite (clinoptilolite) were described well by the pseudo-second-order model (Table 4), whereby the correlation coefficient is 1.000. This type of kinetic model was used to describe the process of adsorption as chemical adsorption (chemisorption) occurs, and it has been widely applied to describe the pollutant adsorption from aqueous solutions [42].

It has been reported that the adsorption capacity of the zeolite depends on the porosity as well as the chemical reaction between the pollutants and the active functional groups [43]. In the current study, the infrared spectra (FT-IR) for zeolite were determined in a range of 400 to 4000 cm^{-1} . The bands appeared at 3634 – 3780 , 1625 , 1024 , 784 , and 709 cm^{-1} (Figure 6). From these obtained results, it is clear that the bands at 3634 – 3780 cm^{-1} and 1625 cm^{-1} confirm the presence of O-H stretching. The FT-IR spectra of clinoptilolite also show a stretching band at 1024 cm^{-1} , which belongs to an asymmetry stretch (AlO or SiO stretching in AlO_4 or SiO_4). Meanwhile, the appeared bands at 784 and 709 cm^{-1} indicate the presence of symmetry stretch (O-Al-O or O-Si-O stretching). The FT-IR results for clinoptilolite showed a change in the band sites or its intensity after the adsorption of ^{226}Ra (Figure 6). Following ^{226}Ra adsorption onto clinoptilolite, the stretching vibration of the AlO or SiO at 1024 cm^{-1} shifted to 1054 cm^{-1} with a lower intensity compared to its corresponding band appeared on clinoptilolite samples before adsorption. Similarly, the stretching vibration of the O-Al-O or O-Si-O stretching at 784 cm^{-1} showed a lower intensity compared to its corresponding band which appeared on clinoptilolite samples before adsorption. Additionally, the OH stretching vibrations at 1625 cm^{-1} and 3634 – 3780 cm^{-1} were diminished following ^{226}Ra adsorption onto clinoptilolite. This suggests

that many interactions with the functional groups of the zeolite may be responsible for contributing to the adsorption process of ^{226}Ra onto natural zeolite.

In this context, different mechanisms could be proposed for ^{226}Ra adsorption on zeolite (Figure 7). It could suggest that the zeolite contains various functional groups of hydroxyl and oxygen, which have the capacity to bind ^{226}Ra via surface complexation, electrostatic attraction, and/or ion exchange.

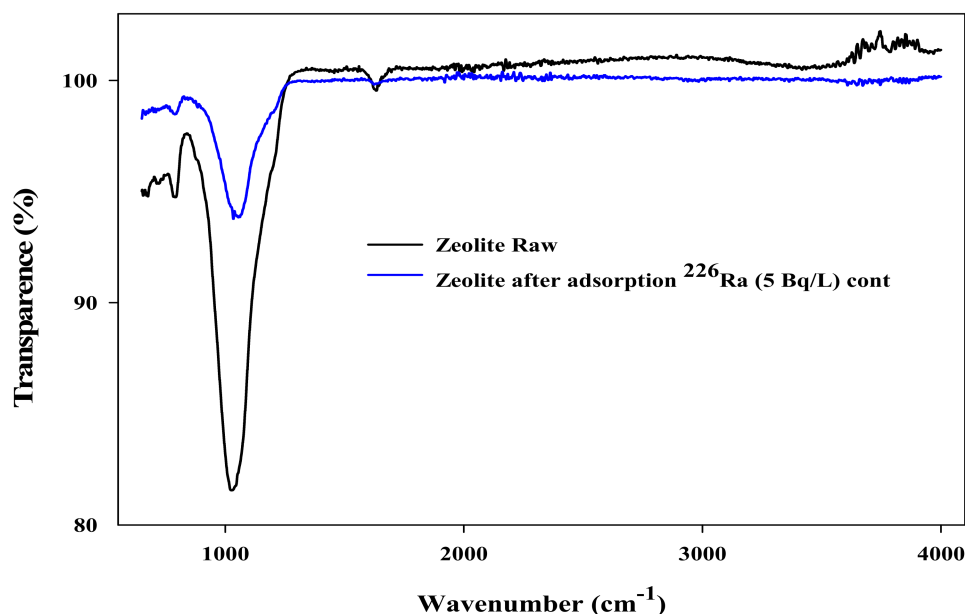


Figure 6. The FT-IR spectrum comparing between the raw zeolite and after ^{226}Ra adsorption onto zeolite.

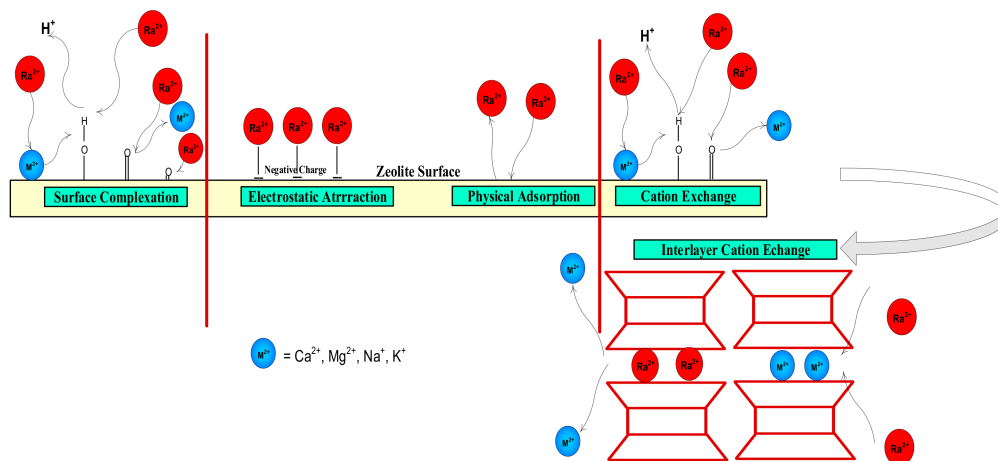


Figure 7. The various proposed mechanisms for the sorption of ^{226}Ra onto zeolite mineral.

4. Conclusions

In this work, an investigation of the adsorption isotherms of ^{226}Ra onto zeolite, montmorillonite, and biochar equilibrium sorption was carried out. Four adsorption isotherm models were studied: Linear, Langmuir, Freundlich, and Temkin isotherms. In addition to the linear model, the Freundlich adsorption model was found to be the best fit. Among the investigated sorbents, zeolite showed a better performance for ^{226}Ra removal from aqueous solutions and groundwater and soil remediation. Kinetic adsorption for the removal of ^{226}Ra from aqueous solution was obtained for the investigated sorbents and fitted to different kinetic models. The results of the kinetic models reveal that the pseudo-second-order model has the best fit for the adsorption of ^{226}Ra onto the three investigated

sorbents, especially zeolite, indicating the chemisorption of the ^{226}Ra onto the sorbents. However, the mechanism of ^{226}Ra adsorption by zeolite, montmorillonite, or biochar is complex and can probably occur by a combination process including sorption processes and/or external mass transfer and intraparticle diffusion through the macropores and micropores. It could be concluded that zeolite is an effective sorbent for the removal of ^{226}Ra from aqueous solution and groundwater and soil remediation.

Author Contributions: Conceptualization, A.R.A.U.; data curation, F.I.A., A.S.A.-F., Y.J.A. and M.I.A.-W.; formal analysis, A.R.A.U., F.I.A., and A.S.A.-F.; funding acquisition, A.R.A.U.; investigation, M.I.A.-W., F.I.A., Y.J.A., Z.Q.A. and A.R.A.U.; methodology, F.I.A., Y.J.A., and A.S.A.-F.; project administration, A.R.A.U.; writing—original draft, F.I.A., Z.Q.A. and A.R.A.U.; writing—review and editing, F.I.A., Z.Q.A., A.S.A.-F., M.I.A.-W., and A.R.A.U. All authors have read and agreed to the published version of the manuscript.

Funding: This research was funded by the Deanship of Scientific Research, King Saud University, under the research group project number RG-1441-515.

Acknowledgments: The authors extend their appreciation to the Deanship of Scientific Research, King Saud University, for funding this work through the research group project RG-1441-515. The authors would like to acknowledge the technical assistance received by the Nuclear Science Research Institute (NSRI) and National Centre for Nuclear Technology (NCNT) at King Abdulaziz City for Science and Technology (KACST) in Riyadh, Saudi Arabia.

Conflicts of Interest: The authors declare no conflict of interest.

References

1. Condomines, M.; Rihs, S.; Lloret, E.; Seidel, J. Determination of the four natural Ra isotopes in thermal waters by gamma-ray spectrometry. *Appl. Radiat. Isot.* **2010**, *68*, 384–391. [[CrossRef](#)] [[PubMed](#)]
2. Moise, T.; Starinsky, A.; Katz, A.; Kolodny, Y. Ra isotopes and Rn in brines and ground waters of the Jordan-Dead Sea Rift Valley: Enrichment, retardation, and mixing. *Geochim. Cosmochim. Acta* **2000**, *64*, 2371–2388. [[CrossRef](#)]
3. Al-Masri, M.; Suman, H. NORM waste management in the oil and gas industry: The Syrian experience. *J. Radioanal. Nucl. Chem.* **2003**, *256*, 159–162. [[CrossRef](#)]
4. IAEA. *Radiation Protection and the Management of Radioactive Waste in the Oil and Gas Industry International Atomic Energy Agency*; Safety Reports Series No.34; IAEA: Vienna, Austria, 2003.
5. Testa, C.; Desideri, D.; Meli, M.; Roselli, C.; Bassignani, A.; Finazzi, P. Determination of uranium, thorium and radium in waters, soils and muds around a uranium mine in decommissioning. *Appl. Radiat. Isot.* **1994**, *45*, 394. [[CrossRef](#)]
6. Barišić, D.; Lulić, S.; Miletić, P. Radium and uranium in phosphate fertilizers and their impact on the radioactivity of waters. *Water Res.* **1992**, *26*, 607–611. [[CrossRef](#)]
7. UNSCEAR. *Sources and Effects of Ionizing Radiation: Sources*; United Nations Publications: New York, NY, USA, 2000; Volume 1.
8. USEPA. *Guidelines for Developmental Toxicity Risk Assessment*; Risk Assessment Forum, U.S. Environmental Protection Agency: Washington, DC, USA, 1991.
9. USEPA. *United States Environmental Protection Agency: Drinking Water Regulations and Health Advisories*; EPA 822-B-96-002; Office of Water, U.S. EPA: Washington, DC, USA, 1996.
10. Alkhomashi, N.; Al-Hamarneh, I.F.; Almasoud, F. Determination of natural radioactivity in irrigation water of drilled wells in northwestern Saudi Arabia. *Chemosphere* **2016**, *144*, 1928–1936. [[CrossRef](#)]
11. Almasoud, F.; Ababneh, Z.Q.; Alanazi, Y.J.; Khandaker, M.U.; Sayyed, M. Assessment of radioactivity contents in bedrock groundwater samples from the northern region of Saudi Arabia. *Chemosphere* **2020**, *242*, 125181. [[CrossRef](#)]
12. Bonotto, D.M.; Bueno, T.O.; Tessari, B.W.; Silva, A. The natural radioactivity in water by gross alpha and beta measurements. *Radiat. Meas.* **2009**, *44*, 92–101. [[CrossRef](#)]
13. Kumar, A.; Karpe, R.; Rout, S.; Gautam, Y.P.; Mishra, M.; Ravi, P.; Tripathi, R. Activity ratios of $^{234}\text{U}/^{238}\text{U}$ and $^{226}\text{Ra}/^{228}\text{Ra}$ for transport mechanisms of elevated uranium in alluvial aquifers of groundwater in south-western (SW) Punjab, India. *J. Environ. Radioact.* **2016**, *151*, 311–320. [[CrossRef](#)]
14. Shabana, E.; Kinsara, A. Radioactivity in the groundwater of a high background radiation area. *J. Environ. Radioact.* **2014**, *137*, 181–189. [[CrossRef](#)]

15. Turhan, Ş.; Özçıtak, E.; Taşkın, H.; Varinlioğlu, A. Determination of natural radioactivity by gross alpha and beta measurements in ground water samples. *Water Res.* **2013**, *47*, 3103–3108. [[CrossRef](#)] [[PubMed](#)]
16. AlEissa, K.A.; Alghamdi, A.S.; Almasoud, F.; Islam, S. Measurement of radon levels in groundwater supplies of Riyadh with liquid scintillation counter and the associated radiation dose. *Radiat. Prot. Dosim.* **2013**, *154*, 95–103. [[CrossRef](#)] [[PubMed](#)]
17. Al-Zubari, W. Sustainable Water Consumption in Arab Countries. *Arab Environ. 8-Sustain. Consum. Better Resour. Manag.* **2015**, 108–113.
18. Al-Hamarneh, I.F.; Alkhomashi, N.; Almasoud, F. Study on the radioactivity and soil-to-plant transfer factor of ²²⁶Ra, ²³⁴U and ²³⁸U radionuclides in irrigated farms from the northwestern Saudi Arabia. *J. Environ. Radioact.* **2016**, *160*, 1–7. [[CrossRef](#)] [[PubMed](#)]
19. Viglasova, E.; Krajnak, A.; Galambos, M.; Roszkopfova, O. *Removal of Uranium from Water Media by Bentonite and Zeolite*; CHÉMIA: Bratislava, Slovak Republic, 2014.
20. Chalupnik, S.; Franus, W.; Wysocka, M.; Gzyl, G. Application of zeolites for radium removal from mine water. *Environ. Sci. Pollut. Res.* **2013**, *20*, 7900–7906. [[CrossRef](#)] [[PubMed](#)]
21. Lumiste, L.; Münter, R.; Sutt, J.; Kivimäe, T.; Eensalu, T. Removal of radionuclides from Estonian groundwater using aeration, oxidation, and filtration. *Proc. Estonian Acad. Sci.* **2012**, *61*, 58–64. [[CrossRef](#)]
22. Wang, S.; Peng, Y. Natural zeolites as effective adsorbents in water and wastewater treatment. *Chem. Eng. J.* **2010**, *156*, 11–24. [[CrossRef](#)]
23. Erenturk, S.; Kaygun, A.K. Removal of ²²⁶Ra from aqueous media and its thermodynamics and kinetics. *J. Radioanal. Nucl. Chem.* **2017**, *311*, 1227–1233. [[CrossRef](#)]
24. Li, H.; Shi, W.-Y.; Shao, H.-B.; Shao, M. The remediation of the lead-polluted garden soil by natural zeolite. *J. Hazard. Mater.* **2009**, *169*, 1106–1111. [[CrossRef](#)]
25. Osmanlioglu, A.E. Treatment of radioactive liquid waste by sorption on natural zeolite in Turkey. *J. Hazard. Mater.* **2006**, *137*, 332–335. [[CrossRef](#)]
26. Ovhal, S.; Butler, I.S.; Xu, S. The Potential of Zeolites to Block the Uptake of Radioactive Strontium-90 in Organisms. *Contemp. Chem.* **2018**, *1*, 1–13.
27. Al-Wabel, M.I.; Al-Omran, A.; El-Naggar, A.H.; Nadeem, M.; Usman, A.R.A. Pyrolysis temperature induced changes in characteristics and chemical composition of biochar produced from conocarpus wastes. *Bioresour. Technol.* **2013**, *131*, 374–379. [[CrossRef](#)] [[PubMed](#)]
28. Al-Hamarneh, I.F.; Almasoud, F. A comparative study of different radiometric methodologies for the determination of ²²⁶Ra in water. *Nucl. Eng. Technol.* **2018**, *50*, 159–164. [[CrossRef](#)]
29. Cooper, E.; Brown, R.; Milton, G. Determination of ²²²Rn and ²²⁶Ra in environmental waters by liquid scintillation counting. *Environ. Int.* **1988**, *14*, 335–340. [[CrossRef](#)]
30. Escobar, V.G.; Tomé, F.V.; Lozano, J.; Sánchez, A.M. Determination of ²²²Rn and ²²⁶Ra in aqueous samples using a low-level liquid scintillation counter. *Appl. Radiat. Isot.* **1996**, *47*, 861–867. [[CrossRef](#)]
31. Prichard, H.M.; Gesell, T.F. Rapid Measurements of ²²²Rn Concentrations in Water with a Commercial Liquid Scintillation Counter. *Health Phys.* **1977**, *33*, 577–581. [[CrossRef](#)]
32. Zouridakis, N.; Ochsenkühn, K.; Savidou, A. Determination of uranium and radon in potable water samples. *J. Environ. Radioact.* **2002**, *61*, 225–232. [[CrossRef](#)]
33. Giles, C.H.; D’Silva, A.P.; Easton, I.A. A general treatment and classification of the solute adsorption isotherm part. II. Experimental interpretation. *J. Colloid Interface Sci.* **1974**, *47*, 766–778. [[CrossRef](#)]
34. Lee, S.-Z.; Allen, H.E.; Huang, C.P.; Sparks, N.L.; Sanders, P.F.; Peijnenburg, W.J.G.M. Predicting Soil–Water Partition Coefficients for Cadmium. *Environ. Sci. Technol.* **1996**, *30*, 3418–3424. [[CrossRef](#)]
35. Rafique, M.I.; Usman, A.R.A.; Ahmad, M.; Sallam, A.; Al-Wabel, M.I. In situ immobilization of Cr and its availability to maize plants in tannery waste–contaminated soil: Effects of biochar feedstock and pyrolysis temperature. *J. Soils Sediments* **2020**, *20*, 330–339. [[CrossRef](#)]
36. Wang, L.; Wang, Y.; Ma, F.; Tankpa, V.; Bai, S.; Guo, X.; Wang, X. Mechanisms and reutilization of modified biochar used for removal of heavy metals from wastewater: A review. *Sci. Total. Environ.* **2019**, *668*, 1298–1309. [[CrossRef](#)] [[PubMed](#)]
37. Houhoune, F.; Khemaissia, S.; Nibou, D.; Chegrouche, S.; Menacer, S. Kinetic study and sorption mechanism of uranium (VI) onto NaY zeolite. In *AIP Conference Proceedings*; AIP Publishing LLC: Melville, NY, USA, 2018; Volume 1994, p. 070008.

38. WHO. Chapter 9 Radiological Aspects. In *Guidelines for Drinking-Water Quality*, 4th ed.; WHO: Geneva, Switzerland, 2011.
39. Misaelides, P. Application of natural zeolites in environmental remediation: A short review. *Microporous Mesoporous Mater.* **2011**, *144*, 15–18. [[CrossRef](#)]
40. El-Naggar, M.; El-Kamash, A.; El-Dessouky, M.; Ghonaim, A. Two-step method for preparation of NaA-X zeolite blend from fly ash for removal of cesium ions. *J. Hazard. Mater.* **2008**, *154*, 963–972. [[CrossRef](#)] [[PubMed](#)]
41. El-Rahman, K.A.; El-Kamash, A.M.; El-Sourougy, M.R.; Abdel-Moniem, N.M. Thermodynamic modeling for the removal of Cs⁺, Sr²⁺, Ca²⁺ and Mg²⁺ ions from aqueous waste solutions using zeolite A. *J. Radioanal. Nucl. Chem.* **2006**, *268*, 221–230. [[CrossRef](#)]
42. Bujdák, J. Adsorption kinetics models in clay systems. The critical analysis of pseudo-second order mechanism. *Appl. Clay Sci.* **2020**, *191*, 105630. [[CrossRef](#)]
43. Mahmoodi, N.M.; Saffar-Dastgerdi, M.H. Zeolite nanoparticle as a superior adsorbent with high capacity: Synthesis, surface modification and pollutant adsorption ability from wastewater. *Microchem. J.* **2019**, *145*, 74–83. [[CrossRef](#)]

Publisher's Note: MDPI stays neutral with regard to jurisdictional claims in published maps and institutional affiliations.



© 2020 by the authors. Licensee MDPI, Basel, Switzerland. This article is an open access article distributed under the terms and conditions of the Creative Commons Attribution (CC BY) license (<http://creativecommons.org/licenses/by/4.0/>).